Atmospheric Dynamics of the Outer Planets

ANDREW P. INGERSOLL

Despite major differences in the solar and internal energy inputs, the atmospheres of the four Jovian planets all exhibit latitudinal banding and high-speed jet streams. Neptune and Saturn are the windiest planets, Jupiter is the most active, and Uranus is a tipped-over version of the others. Large oval storm systems exhibit complicated time-dependent behavior that can be simulated in numerical models and laboratory experiments. The largest storm system, the Great Red Spot of Jupiter, has survived for more than 300 years in a chaotic shear zone where smaller structures appear and dissipate every few days. Future space missions will add to our understanding of small-scale processes, chemical composition, and vertical structure. Theoretical hypotheses about the interiors provide input for fluid dynamical models that reproduce many observed features of the winds, temperatures, and cloud patterns. In one set of models the winds are confined to the thin layer where clouds form. In other models, the winds extend deep into the planetary fluid interiors. Hypotheses will be tested further as observations and theories become more exact and detailed comparisons are made.

THE OUTER PLANETS—JUPITER, SATURN, URANUS, AND Neptune—are fluid objects. There are no continents or oceans to interfere with the flow of gas in the atmosphere. The structures that one sees are fluid structures—patterns in the clouds made visible by condensation of trace constituents. The circulations are powered by solar energy, as on Earth, plus internal energy left over from the formation of the solar system. Small features in the atmospheres usually last for only a few hours or a day, but larger features often last for decades or centuries. An obvious question is why these large atmospheric structures—storms—last so much longer on the outer planets than they do on Earth.

The two Voyager spacecraft, which recently completed their Grand Tour of the outer solar system, revealed much about the dynamics of the atmospheres. Jupiter's latitudinal bands, the zonal jet streams, and the long-lived oval spots were known before Voyager. The intense eddy activity at scales below the resolution of Earth-based telescopes was an important Voyager discovery and served to deepen the mystery surrounding the long-lived ovals and latitudinal bands. The 500-m/s (1800-km/hour) winds of Saturn, three times faster than those of Jupiter, were another important discovery. The existence of latitudinal bands on Uranus, despite that planet's peculiar orientation, showed that planetary rotations, not energy sources, control the patterns of atmospheric circulation. Neptune was a surprise because its wind speeds were greater than any seen elsewhere in the solar system, despite its low solar energy input. The power per unit area that drives Neptune's Great Dark Spot (GDS), for example, is 5% of that which drives the Great Red Spot (GRS) of Jupiter.

This article focuses on the data and the models of the atmospheric circulations. The data come from the Pioneer and Voyager spacecraft and from 300 years of Earth-based telescopic observations. The picture is not complete. Many input parameters of the models—including the abundance of water and other condensables, the degree of coupling to motions in the interior, and the role of small-scale processes—are largely unknown. The models differ in the assumptions made about these parameters. Progress occurs when the model gives a definite output that can be compared to observation. Finding such comparisons is a continuing challenge.

Clouds and Winds

The colored images published after each Voyager encounter (*1–4*) show the patterns and motions of the clouds. The images are processed to bring out details in the images at the cost of exaggerating the colors. In Fig. 1 the four planets are shown to scale at low spatial resolution. Table 1 gives the values of key physical parameters.

The composition and altitude of the clouds are somewhat uncertain. There are a number of condensable species, all present at concentrations less than 1%, and all capable of contributing to the variety of colored clouds. The uncertainties arise because solid and liquid particles do not have definite spectral signatures, and the scattered photons sample a wide range of altitudes within the clouds (*5, 6*).

In general, the atmospheres are mixtures of molecular hydrogen (H_2) and helium, and the visible clouds are ammonia (NH_3) colored by sulfur, phosphorus, and carbon compounds, with high-altitude cirrus clouds of methane (CH_4) at Uranus and Neptune. Ammonium hydrosulfide (NH_4SH) and water are thought to condense at deeper levels on all four planets. Cloud-top pressures are in the range 0.3 to 3 bars. Cloud base is at 5 to 15 bars according to current models, at least on Jupiter and Saturn. There are no sharp boundaries—discontinuities of density, for example—between the atmospheres and the fluid interiors. These low-viscosity fluids are gently stirred by sunlight and by internal heat, but at much lower rates than those on the sun and stars.

Winds are measured by tracking cloud features in sequences of two or more images separated in time. The uncertainty in altitude is a problem when substantial wind shear exists. Another problem is that the clouds sometimes deform and dissipate and perhaps even propagate, like disturbances riding the crest of a wave. These difficulties are reduced by following only the smallest features over

The author is in the Division of Geological and Planetary Sciences, California Institute of Technology, Pasadena, CA 91125.

the shortest time intervals, until the finite resolution of the camera limits the accuracy of the measurement.

Despite the uncertainties, the features generally move as well-defined units that show up best in a motion picture. Sequences from the movies of the GRS of Jupiter and the GDS of Neptune are shown in Figs. 2 and 3, respectively. At the scales shown, there is little evidence of flow vectors crossing other flow vectors, which would occur if the winds were at different altitudes. Such movies bolster the impression that the measured velocities are representative of a single layer near the cloud tops. Besides providing quantitative estimates of velocity, sequences such as Figs. 2 and 3 provide estimates of vorticity and divergence and other more complicated behavior such as merging, dividing, and oscillation of spots.

The profiles of zonal (eastward) velocity versus latitude for all four of the outer planets (*3, 4, 7–10*) are shown in Fig. 4. The winds are measured with respect to a reference frame that rotates with the interior of each planet. The internal periods of rotation are given in Table 1 and are deduced from periodic radio emissions (*11*). It is assumed that the radio emissions are modulated by the magnetic field, which is presumably tied to the electrically conducting interior of each planet. For Saturn the nature of the modulation is obscure, since the magnetic field is almost axisymmetric (*12*).

The zonal velocities do not follow a simple rule. In a prograde jet the features have shorter periods of rotation than the interior, and in a retrograde jet the periods are longer, but in no case is there a reversal of the direction of rotation. Jupiter and Saturn have prograde equatorial jets, whereas Uranus and Neptune have retrograde equatorial jets. Jupiter has many alternating prograde and retrograde jets at mid-latitudes. Saturn's major jets are all prograde. Uranus and Neptune have smoother profiles than Jupiter or Saturn, and Neptune's winds are almost entirely retrograde.

Neptune seems to have the largest wind speeds of any planet in the solar system, according to the data in Fig. 4. The crosses represent the motion of individual bright elements within the larger bright features, like those that flank the GDS in Fig. 3. The elements last only for a few hours, so there are large uncertainties (±60 m/s) in the measured velocity. Those at 18°S seem to overlie the GDS and move at high speed relative to it. Other evidence, from the length of cloud shadows and the appearance of the clouds in different filters, supports the view that the bright clouds are several scale heights above the main cloud deck (*4*). Nevertheless, the high speeds implied by the crosses must be considered preliminary results from the Neptune encounter (*4*) and are still subject to revision. These problems are much less severe at Jupiter and Saturn, where all of the measurements of the wind at a given location tend to give the same result.

The preponderance of prograde winds on Saturn led to speculation that the radio period does not reflect the true period of the interior (*13, 14*), but no alternative theory has been put forward to explain the radio periodicity. The Uranus and Neptune results showed that no two velocity profiles are the same. The large differences between the profiles of Fig. 4 cannot be eliminated by adjusting the reference frames. Our present meager understanding of these differences does not justify abandoning the radio emissions at the best indicator of the internal rates of rotation.

Temperatures and Depth of Circulation

How deep do the zonal winds extend? Is there a level below which the fluid rotates uniformly? These are fundamental questions, but there are no simple answers. At one extreme the zonal winds could be the surface manifestation of differentially rotating fluid cylinders coaxial with the planetary axis of rotation (*15, 16*). At the other

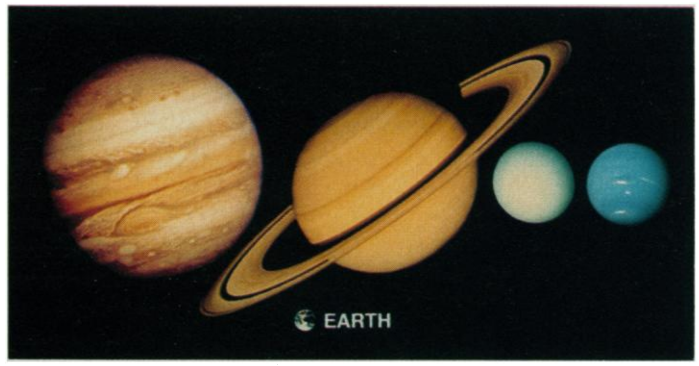

Fig. 1. Color composite of Jupiter, Saturn, Uranus, and Neptune, with Earth for comparison. The relative sizes are accurate, but color and contrast are enhanced to bring out features in the atmospheres. Methane gas, which is relatively abundant on Uranus and Neptune, gives those planets their blue color by selectively absorbing long wavelengths.

extreme, the winds could be confined to a thin weather layer above cloud base, with the interior in solid rotation (*13, 14*). An intermediate case is also possible, in that the winds could have deep roots parallel to the rotation axis but still die out eventually with depth (*16*).

Several approaches to these questions can be taken (*9, 17*). The first is to solve the whole problem on a computer, treating the interior and atmosphere as a single fluid. Fundamental obstacles arise, however, in dealing with fluid motions of vastly different time and space scales. In addition, certain key thermophysical properties are not known well enough to build a definitive model. The second approach is to solve for the motion in the weather layer, treating the interior by means of a lower boundary condition. Different assumptions about temperature gradients and winds, or lack thereof, in the interior lead to different model results. These approaches are discussed in sections below. The third approach, followed here, is to use temperature data to place constraints on the variation of wind with altitude.

The basic observables are the profiles of temperature and zonal velocity as functions of latitude. The latitudinal profiles of emitted infrared (IR) radiation and the equivalent brightness temperatures (*18–20*) are shown in Fig. 5. Table 1 gives the mean pressure at which the physical temperature is equal to the brightness temperature. This occurs at a definite level in the atmosphere, somewhere above the tops of the clouds. Unfortunately, the IR observations do not probe into the clouds. The basic observables are linked by the

Table 1. Physical parameters of the outer planets: f_e is the ratio of infrared emission to absorbed sunlight for the planet as a whole; T_e is the infrared emission expressed as a blackbody temperature; P_e is the mean pressure at which $T = T_e$; H is the pressure scale height RT_e/mg; and c_s is the speed of sound $\sqrt{\gamma RT_e/m}$. Here R is the universal gas constant, m is the mean molecular weight, and $\gamma = 1.4$ is the ratio of specific heats. The asterisks in the Neptune column signify that certain results are preliminary. The numbers in the last six rows are uncertain in the last digit.

Parameter, symbol	Jupiter	Saturn	Uranus	Neptune
Equatorial radius, r_e (10^3 km)	74.1	60.3	25.6	24.8
Rotation period, $2\pi/\Omega$ (hour)	9.92	10.66	17.24	16.11
Equatorial gravity, g (m/s^2)	22.9	9.1	8.8	11.1
Orbital period, $2\pi/\Omega_o$ (year)	11.9	29.5	84.0	164.8
Obliquity of spin axis, i (degree)	3	27	98	29
Helium mole fraction, f_{He}	0.10	0.03	0.15	0.15*
Emitted/absorbed power, f_e	1.7	1.8	1.0	2.7*
Emission temperature, T_e (K)	124	95	59	59*
Emission pressure, P_e (bar)	0.4	0.3	0.4	0.5
Scale height, H (km)	20	39	25	20
Speed of sound, c_s (m/s)	810	705	560	560

thermal wind equation (*21*), which states that the gradient of zonal wind with altitude (wind shear) is proportional to the gradient of temperature with latitude. If the latter is small, the zonal winds must be deep.

Saturn and Neptune are the most clear-cut cases. These planets have extremely strong zonal winds of mostly one sign. In order that these winds decay to zero in a short distance—several scale heights below the cloud tops—the fractional variation of temperature from equator to pole must be large, of order unity, which is contrary to observation. The Voyager imaging team applied this argument to Saturn and concluded that the zonal winds must extend ten scale heights or more below the cloud tops (*2, 16*), if the equator-to-pole

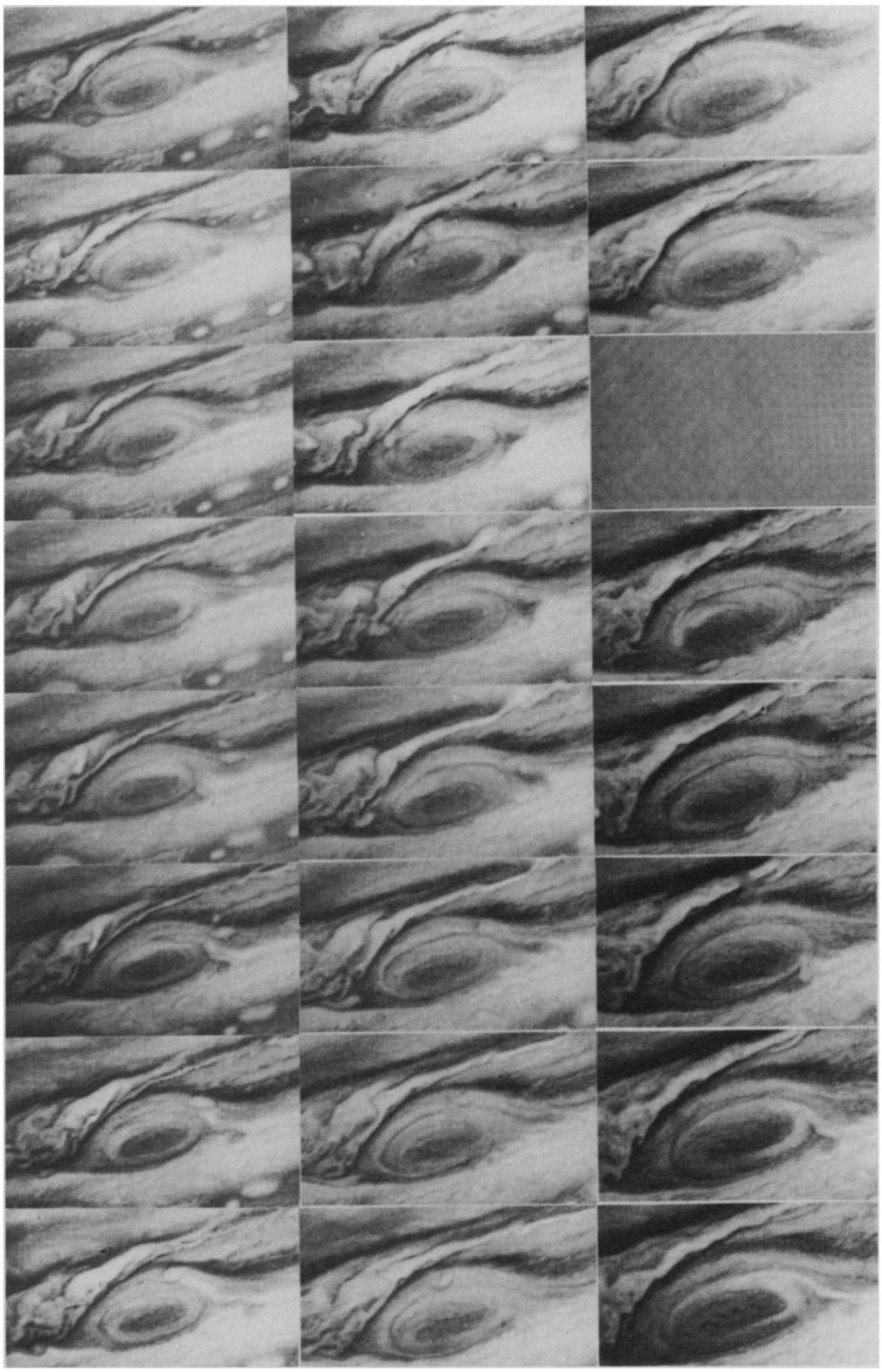

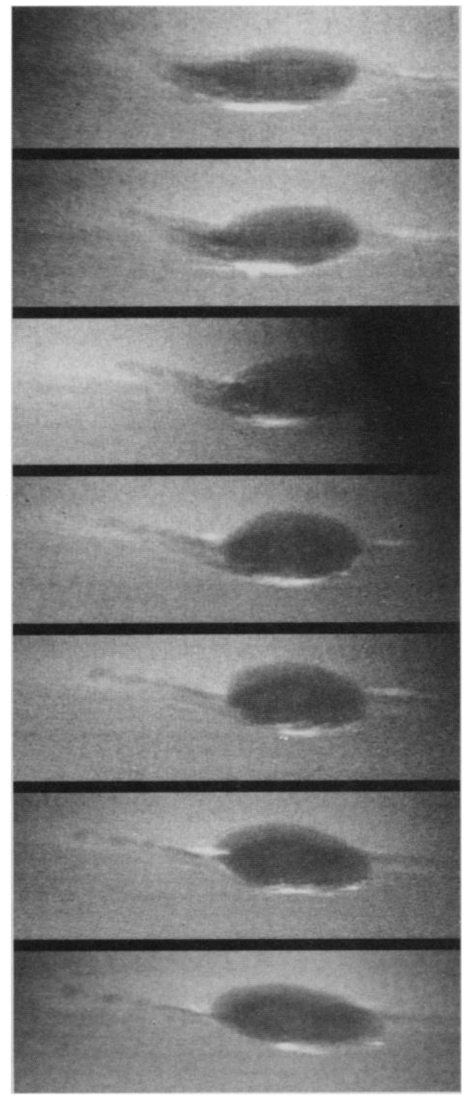

Fig. 2 (left). Time-lapse sequence of the Great Red Spot (GRS) of Jupiter (*1*). Starting from top left, moving down, the sequence shows the counterclockwise flow at intervals of about 20 hours, or two planetary rotations. Smaller spots approach from the east (right), go once around the GRS, and partially merge with it. The GRS is 25,000 km long and 10,000 km wide and has existed for 300 years without changing latitude. The GRS drifts irregularly in longitude at rates of several meters per second. Winds around its periphery exceed 100 m/s. **Fig. 3 (right).** Time-lapse sequence of the Great Dark Spot (GDS) of Neptune (*4*). The GDS and the GRS have the same size relative to the planets and occupy nearly the same latitudes. They both rotate counterclockwise (anticyclonic in the southern hemisphere), but the GDS stretches and contracts as it rotates.

temperature difference is no more than 4% at all levels. A weakness of this argument is that the temperatures are measured above the clouds, whereas the wind shears depend on the temperature gradients at all altitudes. Another weakness is that molecular-weight gradients can mask the effects of temperature gradients, and the former are not well known. The counterargument is that the planetary interiors are thought to be more homogeneous with respect to composition and temperature than the atmospheres. The lack of strong latitudinal gradients in the atmospheres is evidence against large wind shears, implying that the winds are deep.

What processes could account for the near uniformity of temperature—the small equator-to-pole temperature differences on all of the outer planets? On Earth, absorption of sunlight at low latitudes maintains a difference of order 30 K despite the moderating effect of the circulation, which tends to homogenize the atmosphere. Models of the Jovian circulation that are based on analogy with Earth, in which a thin weather layer rests on a thermally insulating solid, give equator-to-pole temperature differences from 3 to 30 K (*14, 22*). Only the lower limit is even marginally compatible with the observations, which at least sample the top of the weather layer. Pioneer 11, the only spacecraft to fly over the poles of Jupiter, found the poles to be slightly warmer than the equator just above the tops of the clouds (*18*). Voyager found the poles of Uranus to be slightly colder than the equator (*20*), although the poles receive the most sunlight. Something appears to be missing from the terrestrial-analog models.

The obvious weakness is the lower boundary condition. The interior probably resembles a thermal conductor more than it does an insulator, for example (*23*). Internal heat drives convection currents that maintain an adiabatic state, at least up to cloud base.

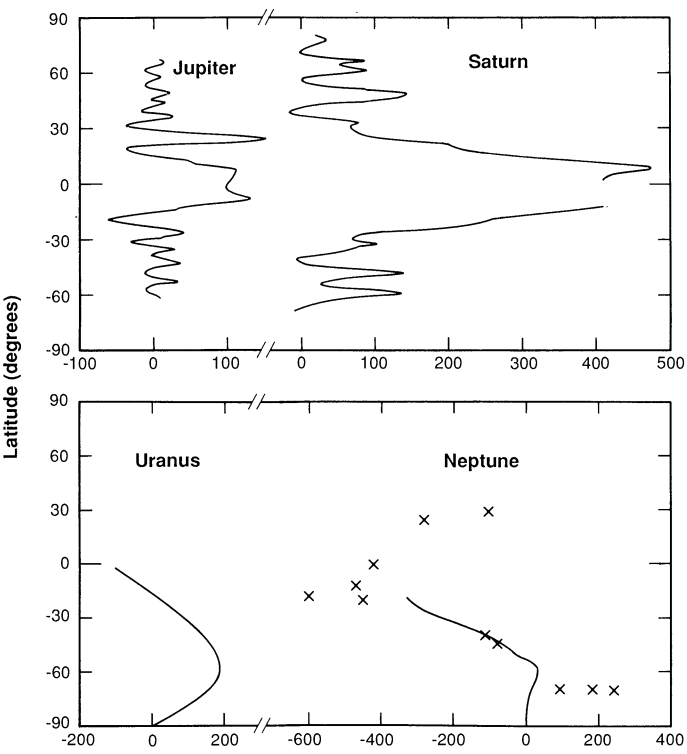

Fig. 4. Zonal velocity versus latitude for the four outer planets (*3, 4, 7–10*). Velocities are measured relative to the planetary interiors, whose rotations are inferred from periodic radio emissions. The measurement involves tracking clouds in sequences of images, usually at intervals of one planetary rotation. Note that the scale for Uranus and Neptune is different from that for Jupiter and Saturn. The crosses for Neptune are high-speed motions measured over intervals of 1 or 2 hours.

Fig. 5. Emitted infrared flux and equivalent brightness temperatures versus latitude for the four outer planets (*18–20*). The radiation is emitted, on average, from the 0.3- to 0.5-bar pressure levels (Table 1). The equator-to-pole temperature differences are small. The largest temperature gradients occur at the extrema of the zonal velocity profile (Fig. 4).

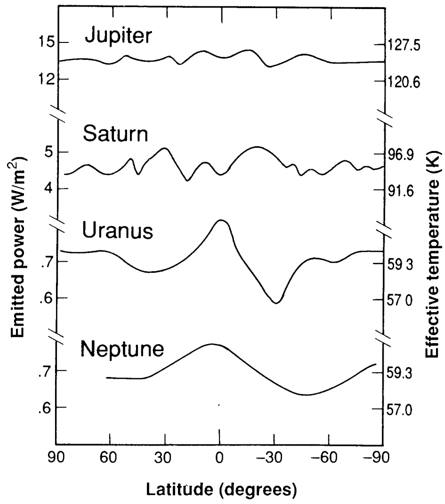

An adiabatic state has temperature equal to a constant independent of latitude on each constant-pressure surface. The convection currents maintain this state despite the uneven distribution of absorbed sunlight because the interior is heated from below and has much more mass than the atmosphere. The thin weather layer is effectively short-circuited by the deep interior, according to this hypothesis (*23*).

A complete model of the weather layer, from cloud base to cloud top, requires a better knowledge of composition, cloud physics, and solar energy deposition than we now have. For example, simple models of the Uranian atmosphere (*22, 24*), analogous to energy-budget climate models of Earth (*22, 25*), give good agreement for the large-scale temperature structure of Fig. 5 but fail to explain the small-scale structure. Treating the interior as a perfect thermal conductor (*24*) accounts for the lack of equator-to-pole temperature contrast, but it does not account for small-scale oscillations of the curves in Fig. 5. Something is still missing.

The Voyager IRIS (infrared spectrometer) team, which made the IR measurements, noticed that the temperature gradients associated with the oscillations occur at the latitudes of the zonal jets—the extrema of the zonal velocity profile. The sign of the correlation indicates that the zonal jets decay with height, at least at the measured altitudes above the tops of the clouds. Finding no radiative process that would produce the temperature oscillations, the IRIS team proposed a dynamical mechanism (*19, 20*). The zonal jets are driven by unspecified processes occurring within and below the weather layer. Above the clouds, frictional drag on the zonal jets causes them to decay with height and at the same time drives a meridional circulation that maintains the temperature oscillations. The model offers a self-consistent explanation for the correlation between the temperature gradients and velocity extrema (Figs. 4 and 5). It does not explain where the zonal jets get their energy or how deep they go. In general, use of the thermal wind equation provides useful constraints but no definitive estimates of the depth of the circulation.

Vorticity as a Probe of Vertical Structure

The second approach mentioned above is to model the dynamics of the weather layer by treating the interior by means of a lower boundary condition. One can either guess at the correct lower boundary condition, using some theoretical intuition about the interior, or one can try to infer it from the data. Velocity data in particular allow some interesting inferences.

One fairly general lower boundary condition treats the interior as an infinitely deep, adiabatic fluid with a steady zonal velocity that could depend on latitude. Solid rotation of the interior is a special case. The adiabaticity and great depth ensure that the prescribed zonal velocity of the interior remains steady regardless of what happens in the weather layer. The zonal velocity profile for the interior enters in the dynamics of the weather layer as an equivalent bottom topography.

The dynamics involves the principle of conservation of potential vorticity (*21*). Potential vorticity is proportional to angular momentum about a vertical axis—a constant for each fluid element. As the layer thins or thickens, the moment of inertia about the vertical axis increases or decreases, and the fluid element spins slower or faster. Here "spin" includes a part due to the velocity relative to the planet and a part due to the vertical component of the planet's angular velocity. For a thin fluid layer on a rotating planet, the expression for potential vorticity is $q = (\zeta + f)/h$. Here, ζ is the vertical component of relative vorticity $\nabla \times \mathbf{v}$, where $\mathbf{v}$ is velocity measured in the planet's rotating frame; $f = 2\Omega \sin \phi$ is the planetary vorticity, where Ω is the planet's angular speed of rotation and ϕ is latitude; h is the thickness of the fluid layer. If the flow is adiabatic (specific entropy conserved following the motion), and the atmosphere is stably stratified (specific entropy increasing upward such that the temperature lapse rate is subadiabatic), then the specific entropy surfaces and material surfaces coincide and h is the mass per unit area between surfaces of constant specific entropy.

The weather layer has negligible effect on the interior because its thickness is so much less than that of the interior. When the interface between them moves up and down, causing order-unity changes in the upper (weather-layer) thickness, the fractional changes in the lower (interior) thickness remain small. The vorticity of the interior does not change. This argument was first applied to Jupiter by assuming that the interior rotates uniformly (*26*) and was later extended to include an arbitrary zonal velocity (*27, 28*) in the interior.

Conservation of potential vorticity is used to probe the weather layer and to determine if zonal winds occur at its base (*29, 30*). This approach uses measurements of ζ and knowledge of f to find h. Vertical structure is simplified so that the weather layer is treated as a single homogeneous fluid of constant properties (constant specific entropy, for example). Zonal jets in the interior produce variations in the height of constant-pressure surfaces at the base of the weather layer. Since the motion is steady and zonal, the pressure gradients are latitudinal and the weather layer "feels" a series of rigid hills and valleys with crests running east-west. Thus the effect of zonal flow in the interior is to add east-west bottom topography to the weather layer, whose dynamics is described by the familiar shallow-water equations (*31*). These are the equations of motion of a homogeneous (constant-density) fluid moving horizontally in a gravitational field, with pressure related to the height of the upper free surface.

Measuring the bottom topography requires finding places where the fluid elements cross latitude lines. Jupiter's GRS at 22°S and the

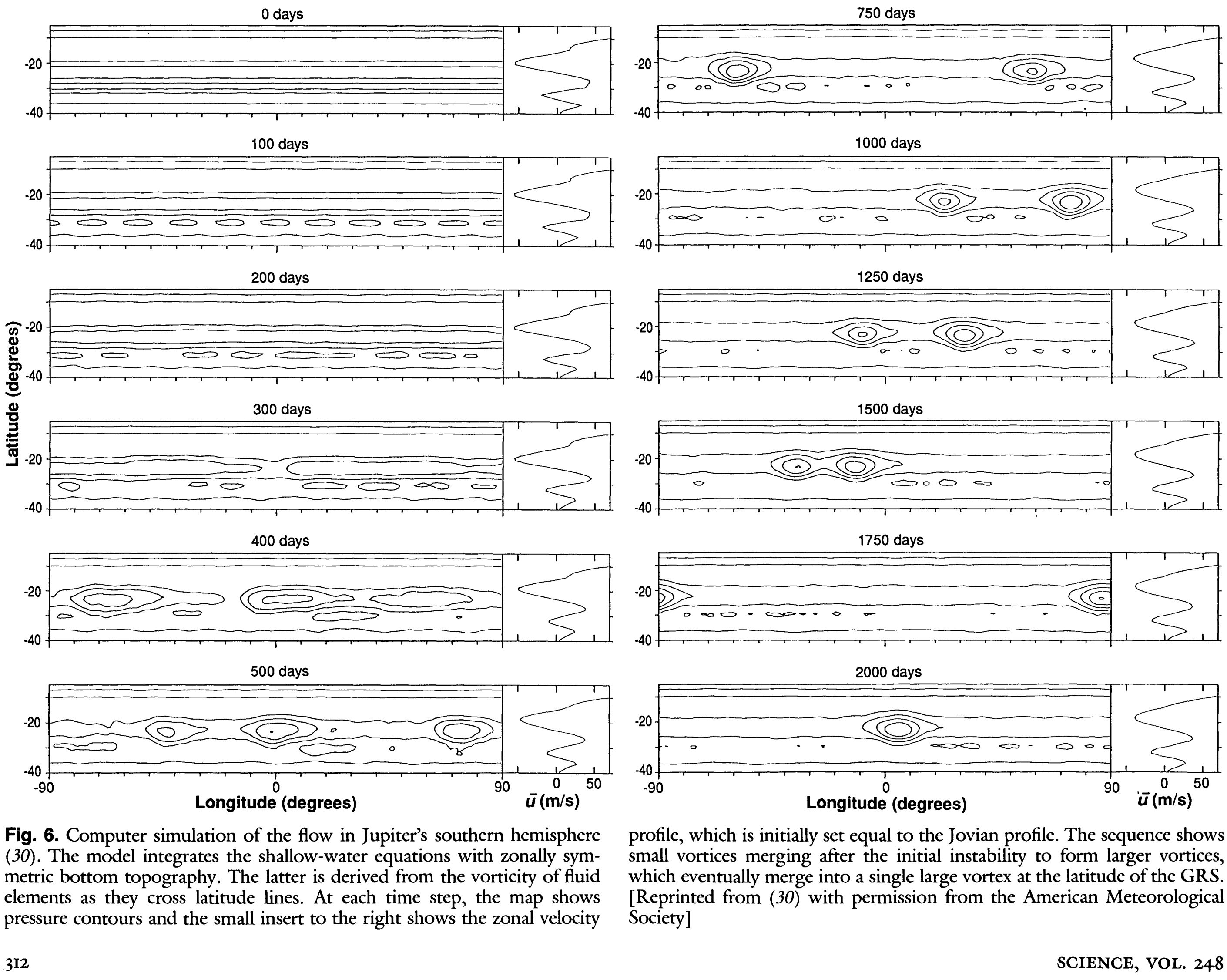

Fig. 6. Computer simulation of the flow in Jupiter's southern hemisphere (*30*). The model integrates the shallow-water equations with zonally symmetric bottom topography. The latter is derived from the vorticity of fluid elements as they cross latitude lines. At each time step, the map shows pressure contours and the small insert to the right shows the zonal velocity profile, which is initially set equal to the Jovian profile. The sequence shows small vortices merging after the initial instability to form larger vortices, which eventually merge into a single large vortex at the latitude of the GRS. [Reprinted from (*30*) with permission from the American Meteorological Society]

white ovals at 33°S provide the best locations. One measures the two-dimensional velocity field around each oval, takes its curl to get ζ, and takes line integrals to get the trajectories of fluid elements. Each element traces out a different path across the topography. Fractional changes of h are inferred from the fractional changes of $(\zeta + f)$. Choosing a single unknown number related to the mean thickness of the weather layer and its density relative to that of the interior allows one to solve for the thickness everywhere. The contribution of the upper free surface height is subtracted off, leaving the height of the bottom topography as a function of latitude.

The results of this observational study (*29, 30*) do not fit any of the theoretical hypotheses (*27, 32, 33*) that had been advanced concerning motion in Jupiter's interior. In these theories as well as in the observational study, the weather layer is treated as a single homogeneous fluid. Although the model is restrictive, varying the mean thickness of the weather layer does not alter the conclusion. The interior is not in solid rotation at the radio rate or at any other rate (*32*). The zonal velocity profile for the interior is not equal to the profile for the cloud tops (*27*), although there are some similarities. The combination $(\zeta + f)/h$ for the zonal flow in the weather layer is not a constant independent of latitude (*33*). In fact, the gradient of $\bar{q}$ with respect to latitude changes sign, and is strongly negative at 20°S and at 33°S, where the overbar refers to the zonal flow far away from the ovals. Such sign reversals are usually a sign of instability (*34*). The observations suggest that the zonal flow in the weather layer is unstable.

Earlier observational studies (*7–10*) focused on the barotropic stability criterion, which states that the flow is stable if $\beta - \bar{u}_{yy}$ does not change sign. Here β is df/dy where y is the northward coordinate, and $\bar{u}_{yy}$ is $-d\bar{\zeta}/dy$, where $\bar{\zeta}$ is $-d\bar{u}/dy$, the vorticity of the zonal flow. This criterion involves the gradient of the numerator of $\bar{q}$, since $\bar{q} = (\bar{\zeta} + f)/h$. The earlier studies established that $\beta - \bar{u}_{yy}$ is negative at the latitudes of the westward jets, including those at 20°S and 33°S. At other latitudes $\beta - \bar{u}_{yy}$ is positive. Thus the barotropic stability criterion is violated near the westward jets. The new studies (*29, 30*) are more general because they include the effects of h. In fact, the gradients of $\bar{\zeta} + f$ and h tend to work together, reinforcing the conclusion that $d\bar{q}/dy$ is negative near the westward jets.

These conclusions depend on the applicability of a single-layer model to the motions at cloud-top altitudes. It would be more realistic to treat the weather layer as a continuum with variable properties. However, the vertical profiles of temperature, radiative heating, and condensable species are uncertain. Instead of one free parameter (the mean thickness of the weather layer), there would be many. Three-dimensional models of isolated vortices in laboratory shear flows have been quite successful (*35*), but in these cases the vertical profiles are known. For the outer planets, one can perhaps assume that the vertical structure follows a moist adiabat (*28, 36*), but the water abundance remains a major unknown. For the moment, the shallow-water equations are matched to the observations. They provide a means of investigating the dynamics of the outer planet atmospheres without having the number of free parameters exceed the number of independent measurements.

Shallow-Water Models of the Dynamics

The preceding section described the use of a single-layer model (shallow-water equations with zonally symmetric bottom topography) to invert a set of observations. This section describes a set of time-dependent numerical simulations that use the derived topography as input to the single-layer model (*30*). The model is also run with topographies that are based on theoretical hypotheses about the zonal flow in the interior (*27, 32, 33*). The aim is to see which bottom topographies reproduce observed features of the circulation, including vortex formation, oscillations, pairings, mergers, and other time-dependent behavior (Figs. 2 and 3). The model has been run only for Jupiter, because the observational data are better than for the other outer planets.

A run of the shallow-water equations with the derived bottom topography (*30*) is shown in Fig. 6. Artificial barriers are placed at 5°S and 40°S because the topography is unknown outside this range. The flow is assumed to be periodic in longitude with period 180°. Contours of free-surface height (pressure) are shown at time intervals indicated in Earth days. The rotation period and radius are appropriate to Jupiter. The mean zonal velocity profile in the weather layer is shown at right. Initially it is equal to the velocity profile observed in Jupiter's atmosphere.

The initial profile is unstable. It breaks up into a series of eddies, which merge until there are only three large eddies at t = 500 days and only two large eddies at t = 750 days. These finally merge at t = 1600 days, leaving a single large vortex at the same latitude as Jupiter's GRS. The sign of the vortex, its strength, size, and longitudinal drift rate all closely match those of the GRS. Runs up to 10 years show no further changes in the single large vortex at 22°S. Smaller vortices are also present at 33°S, but they are lost in the coarse contouring of Fig. 6. This latitude is the same as that of Jupiter's three white ovals, which are about one-third the size of the GRS and resemble it in most respects. The model is consistent with the observations (*37*) that the stable vortices are mostly anticyclonic (sign of ζ opposite to the sign of f) and form in anticyclonic shear zones (eastward velocity increasing toward the pole).

The model demonstrates that vortices will form spontaneously at the right latitudes when the right velocity and bottom topography are used as input. A weakness of the model is that it does not account for the zonal velocity or the topography, except that the latter is meant to represent the pressure associated with zonal flow in a deep lower layer—the interior. More significantly, the zonal flow in the weather layer is unstable (the model does not allow the zonal flow in the interior to be unstable). To keep the flow going, the model uses an artificial Rayleigh friction term—an east-west drag force that is trying to relax the zonal velocity profile to the observed one with a time constant of 400 days. Models without the drag term tend to run down a little more; the zonal flow gives up more of its energy to the vortex when energy is conserved. The rationale for the drag force is that its time constant is long compared to the dynamical time constant $1/\zeta$, which is less than 1 day.

If the right bottom topography, or one very close to it, were the only one that gave vortices forming spontaneously at the latitudes of the Jovian vortices, then the forward numerical integration would support the inversion of the data from which the topography was derived. In reality, all of the topographies give stable vortices. Of the four studied (*30*), two make the zonal flow stable and two leave it unstable. The derived topography leaves it unstable, as does the flat topography associated with solid rotation in the interior (*32*). The wavy topography associated with the zonal flow in the interior that matches that in the weather layer (*27*), and the topography associated with constant $\bar{q}$ (*33*), both give stable zonal flows. The vortices form spontaneously as in Fig. 6 when the zonal flow is unstable, but some kind of artificial force is needed to maintain the unstable zonal flow. Isolated vortices also form spontaneously in certain laboratory experiments (*38, 39*) when a zonal flow is maintained in an unstable state.

Without friction, the stable zonal flows and the vortices go on forever. A small amount of friction causes the vortices to decay unless they are artificially fed with a steady supply of smaller vortices. The smaller vortices do not arise spontaneously when the zonal flow is stable. In other words, the shallow-water models require a source of energy—either an artificial drag term to keep the zonal flow going or an artificial source of small vortices to keep the large ones well fed.

Undoubtedly, future numerical simulations will have multiple degrees of freedom in the vertical (*28*) without using an Earth-like lower boundary condition (*14, 32*). The models will simulate the life cycle of the smaller eddies, which may be the primary convective elements that harness the solar and internal energy. Successful models will simulate the way vortices merge and interact (*37*) and should account for the existence of vortices at all sizes, with diameters ranging from less than 1000 km to the size of the GRS (*37*). The models might explain why the largest spot on Saturn is only 20% the size of the GRS and why Uranus has almost no spots at all. Finally, the simulations will address the oscillations of vortices, like those of Neptune's GDS (Fig. 3) and the so-called brown barges of Jupiter (*40*). The goal is to find the correct model, using the observations as a test.

What Maintains the Zonal Flow?

The most fundamental question is still unanswered. The magnitude, width, and direction of the zonal jets are unexplained. The differences among the zonal flows on the four outer planets are large and are not well understood. The zonal flow at the cloud tops and beneath the clouds are critical for the formation and stability of the long-lived vortices, yet no theory accounts for the properties of these zonal flows.

The traditional view (*26, 36, 41, 42*) is that the zonal jets are shallow and owe their existence to differential heating within the clouds. For instance, frictional drag near the base of the clouds might set up a meridional circulation that concentrates moisture at certain latitudes depending on the sign of the vorticity. An anticyclonic latitude has divergence within the clouds and convergence beneath the clouds, so the anticyclones are preferentially heated from below by latent heat release. Such heating is what sustains them, since the anticyclones are warm-core structures (the thermal wind equation says that as altitude increases the flow becomes increasingly anticyclonic around a warm-core structure and increasingly cyclonic around a cold-core structure). The traditional view is supported by evidence of well-developed clouds at the anticyclonic latitudes and holes in the clouds at the cyclonic latitudes (*43*).

One problem with the traditional view is that it does not explain the latitudinal banding. The mechanisms work equally well for circular spots as for linear bands. The model is similar, in fact, to a terrestrial hurricane model, but with a deep, moisture-laden atmosphere replacing the terrestrial ocean. Another problem is that the model is sensitive to certain processes such as frictional drag, low-level convergence, and latent heat release that may not operate as advertised. A third problem is that the model works poorly for Saturn and Neptune, whose ultrahigh-speed winds are difficult to reconcile with thin-layer models. The model may be correct for Jupiter, but it is difficult to test without better constraints from theory and observation.

The more recent view (*7, 15, 44*) has many of the same problems. It holds that the zonal jets get their energy from the eddies, which get their energy from buoyancy. This two-stage process is known to operate in Earth's atmosphere. Voyager wind data suggest that it may operate on Jupiter (*7*), but the eddy wind data are subject to large errors, and the models have many free parameters.

The Voyager imaging team used global maps of 10,000 velocity vectors collected from image pairs one rotation apart at resolutions of about 60 km/pixel (*7*). The vectors are separated into latitude bins 1° wide, and the mean eastward and northward velocity components $\bar{u}$ and $\bar{v}$ are determined for each bin. The values of $\bar{u}$ define the mean zonal velocity profile of Fig. 4. The values of $\bar{v}$ are small and not statistically significant. The means are subtracted from each vector to get the eddy wind components u' and v'. By definition, the means of u' and v' for each bin are zero. The important quantity is the Reynolds stress $\overline{u'v'}$, which is the average for the bin of the northward transport of eastward momentum by the eddies. The Reynolds stress is defined at each latitude and is compared to $d\bar{u}/dy$ at the latitude. If $\overline{u'v'}$ has the same sign as $d\bar{u}/dy$ at most latitudes, then the eddies are transferring their kinetic energy into the zonal jets.

The result of this analysis (7) is shown in Fig. 7. The ordinate is latitude. The left-hand curve is $d\bar{u}/dy$, and the center and right-hand curves are $r(u',v')$ from Voyager 1 and Voyager 2, respectively. Here $r(u',v')$ is the correlation coefficient, $\overline{u'v'}$ divided by the standard deviations of u' and v' for the latitude. For the planet as a whole the standard deviations of u' and v' are 10 and 6 m/s, respectively. Figure 7 shows that the correlation coefficients are of order 0.3, and that the sign of $r(u',v')$ tends to be the same as that of $d\bar{u}/dy$. The implied rate of energy transfer is enough to double the kinetic energy of the zonal jets in 75 days. If such transfer is occurring over a layer 2.5 bars deep, the transfer rate is 2.3 W/m^2, or 15% of the total thermal energy flux at Jupiter. For Earth, the same term in the mechanical energy cycle is only 0.1% of the total thermal flux. Either Jupiter is much more efficient than Earth in converting thermal energy to mechanical energy, or else the measurement is misleading.

One problem with the measurement is that the eddies are poorly resolved in the images. Selection of features suitable for tracking

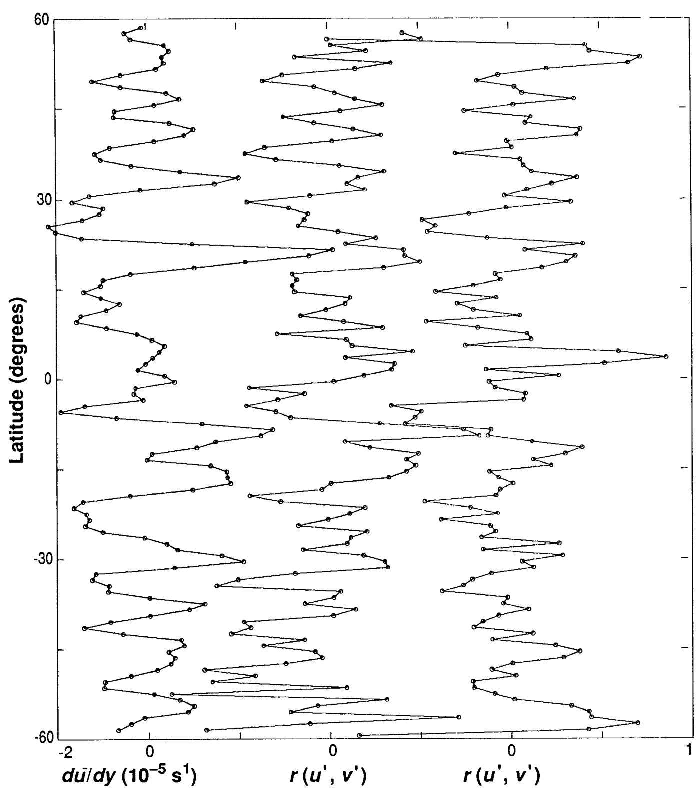

Fig. 7. Comparison of the zonal velocity gradient $d\bar{u}/dy$ (left) with the eddy correlation coefficient $r(u',v')$. The center and right curves are from Voyager 1 and Voyager 2, respectively (7). At most latitudes $r(u',v')$ and $d\bar{u}/dy$ have the same sign, indicating that kinetic energy is being transferred from the eddies to the zonal flow through the Reynolds stress term. [Reprinted from (7) with permission from the American Geophysical Union]

could introduce a bias. For example, sampling only the northeast and southwest quadrants of a clockwise circular eddy would yield a negative estimate for $\overline{u'v'}$ even though the true value is zero (*45*). Another problem is that the net effect of the eddies on the mean winds includes energy transfers that cannot be determined from the Voyager data. These transfers involve the mean meridional velocity $\bar{v}$ and the eddy temperature fluctuations T', neither of which are known.

Although the observations refer to eddies near the tops of the clouds, the mechanism could operate at any level. Eddies in the interior, driven by the internal energy flux, could have Reynolds stresses that pump energy into differentially rotating coaxial cylinders (*15*). Similar mechanisms are thought to occur in the sun and stars, although recent observations from helioseismology show that the solar rotation rate is not constant on cylinders (*46*). Convective eddies, which use latent heat to carry the energy flux upward, might be producing the Reynolds stress in the clouds of the Jovian planets. The movies of Jupiter's atmosphere (*47*) show many phenomena that look like convection—sudden appearances and rapid growth of bright circular spots followed by entrainment and dispersal in the zonal shear flow. The eddies might be produced by baroclinic instability (*44*), which releases stored potential energy associated with horizontal gradients of temperature. The problem with the latter mechanism is that the only temperature gradients seem to be associated with the jets (Fig. 5), and the jets cannot maintain themselves. A separate source, like sunlight, could maintain a temperature difference between equator and poles, but the data show little evidence for such differences.

Implications for the Future

The real surprise about the eddy winds on Jupiter is not that the components u' and v' are correlated. Such correlation is expected for eddies in a shear flow provided that the eddies have a separate energy source like buoyancy. The surprise is that the eddies are so energetic, considering that the radiated power per unit area is only 14 W/m^2 compared with Earth's 240 W/m^2. The dissipation rate U^3/L, computed from the eddy velocity U and eddy length scale L, is also about 2.2 W/m^2 (provided $U = 6$ m/s and $L = 1000$ km) if the dissipation is spread over a layer 2.5 bars deep. These large energy transfers and large eddy winds suggest that the Jovian atmospheres are more efficient as heat engines than the Earth. They can harness a large fraction of their thermal power and convert it to kinetic energy. Also, the large zonal wind speeds, particularly those on Saturn and Neptune, suggest that the Jovian atmospheres are able to store kinetic energy with less dissipation than on Earth. Even among themselves, the ability of the Jovian planets to store kinetic energy varies widely, and is almost inversely related to the thermal energy input. The surprising result is that Earth has the slowest wind speeds of any planet in the solar system, although it absorbs and radiates more power per unit area than any other planet with an atmosphere.

What happens next? The Galileo mission includes a probe that will enter the atmosphere of Jupiter near the equator, sending back information about composition, temperature, winds, clouds, electrical activity, light levels, and IR radiation to a depth of perhaps 20 bars. The Galileo orbiter will spend 2 years around Jupiter, from 1995 to 1997, obtaining high-resolution motion pictures of convective regions, shear zones, waves, and turbulence. It will peer into the clouds with instruments that range across the electromagnetic spectrum. The Cassini orbiter is scheduled to image Saturn at ultraviolet, visible, infrared, and radio wavelengths during the years 2002 to 2006. These measurements will constrain the input parameters of the theoretical models and will provide quantitative measurements for comparison with model output. The assumption behind all of this activity is that by studying the skin of the onion in all its detail, we can finally understand the onion and all of its layers. This is standard operating procedure for geophysicists and astronomers. For atmospheric dynamicists, it is a new way of doing business.

REFERENCES AND NOTES

1. B. A. Smith *et al.*, *Science* **204**, 951 (1979); B. A. Smith *et al.*, *ibid.* **206**, 927 (1979).
2. B. A. Smith *et al.*, *ibid.* **212**, 163 (1981); B. A. Smith *et al.*, *ibid.* **215**, 504 (1982).
3. B. A. Smith *et al.*, *ibid.* **233**, 43 (1986).
4. B. A. Smith *et al.*, *ibid.* **246**, 1422 (1989); H. B. Hammel *et al.*, *ibid.* **245**, 1367 (1989).
5. T. Gehrels and M. S. Matthews, Eds., *Saturn* (Univ. of Arizona Press, Tucson, 1984).
6. R. G. Prinn *et al.*, in (*5*), pp. 88–149; M. G. Tomasko *et al.*, in (*5*), pp. 150–194; K. H. Baines and J. T. Bergstralh, *Icarus* **65**, 406 (1986).
7. R. F. Beebe *et al.*, *Geophys. Res. Lett.* 7, 1 (1980); A. P. Ingersoll *et al.*, *J. Geophys. Res.* **86**, 8733 (1981).
8. S. J. Limaye *et al.*, *J. Atmos. Sci.* **39**, 1413 (1982); S. J. Limaye, *Icarus* **65**, 335 (1986).
9. A. P. Ingersoll *et al.*, in (*5*), pp. 195–238.
10. L. A. Sromovsky *et al.*, *J. Geophys. Res.* **88**, 8650 (1983).
11. A. C. Riddle and J. W. Warwick, *Icarus* **27**, 457 (1976); M. L. Kaiser *et al.*, in (*5*), pp. 378–415; M. D. Desch *et al.*, *Nature* **322**, 42 (1986); J. W. Warwick *et al.*, *Science* **246**, 1498 (1989).
12. J. E. P. Connerney *et al.*, in (*5*), pp. 354–377.
13. M. Allison and P. H. Stone, *Icarus* **54**, 296 (1983).
14. G. P. Williams, *J. Atmos. Sci.* **36**, 932 (1979); *Adv. Geophys.* **28**, 381 (1985).
15. F. H. Busse, *Astrophys. J.* **159**, 629 (1970); *Icarus* **29**, 255 (1976); *Geophys. Astrophys. Fluid Dyn.* **23**, 153 (1983).
16. A. P. Ingersoll and D. Pollard, *Icarus* **52**, 62 (1982); A. P. Ingersoll and R. L. Miller, *ibid.* **65**, 370 (1986).
17. F. M. Flasar, *ibid.*, p. 280; M. Allison *et al.*, in *Uranus*, J. Bergstralh and E. Miner, Eds. (Univ. of Arizona Press, Tucson, in press).
18. A. P. Ingersoll *et al.*, in *Jupiter*, T. Gehrels, Ed. (Univ. of Arizona Press, Tucson, 1976), pp. 197–205.
19. J. A. Pirraglia *et al.*, *Icarus* **59**, 169 (1984); P. J. Gierasch *et al.*, *ibid.* **67**, 456 (1986); B. J. Conrath and J. A. Pirraglia, *ibid.* **53**, 286 (1983); R. A. Hanel *et al.*, *ibid.*, p. 262.
20. F. M. Flasar *et al.*, *J. Geophys. Res.* **92**, 15,011 (1987); B. Conrath *et al.*, *Science* **246**, 1454 (1989).
21. J. R. Holton, *An Introduction to Dynamic Meteorology* (Academic Press, New York, ed. 2, 1979).
22. P. H. Stone, *J. Atmos. Sci.* **29**, 405 (1972); *Space Sci. Rev.* **14**, 444 (1973).
23. A. P. Ingersoll, *Icarus* **29**, 245 (1976); ——— and C. C. Porco, *ibid.* **35**, 27 (1978).
24. J. Friedson and A. P. Ingersoll, *ibid.* **69**, 135 (1987).
25. M. I. Budyko, *Tellus* **21**, 611 (1969); W. D. Sellers, *J. Atmos. Sci.* **12**, 241 (1973).
26. P. J. Gierasch *et al.*, *Icarus* **40**, 205 (1979).
27. A. P. Ingersoll and P. G. Cuong, *J. Atmos. Sci.* **38**, 2067 (1981).
28. R. K. Achterberg and A. P. Ingersoll, *ibid.* **46**, 2448 (1989).
29. T. E. Dowling and A. P. Ingersoll, *ibid.* **45**, 1380 (1988).
30. ———, *ibid.* **46**, 3256 (1989).
31. A. E. Gill, *Atmosphere-Ocean Dynamics* (Academic Press, New York, 1982); J. Pedlosky, *Geophysical Fluid Dynamics* (Springer-Verlag, New York, ed. 2, 1987).
32. G. P. Williams and T. Yamagata, *J. Atmos. Sci.* **41**, 453 (1984); G. P. Williams and R. J. Wilson, *ibid.* **45**, 207 (1988).
33. P. S. Marcus, *Nature* **331**, 693 (1988).
34. P. Ripa, *J. Fluid Mech.* **126**, 463 (1983).
35. P. L. Read and R. Hide, *Nature* **308**, 45 (1984); P. L. Read, *Icarus* **65**, 304 (1986).
36. A. Barcilon and P. J. Gierasch, *J. Atmos. Sci.* **27**, 550 (1970); P. J. Gierasch *et al.*, *J. Geophys. Res.* **92**, 15,019 (1987).
37. M.-M. Mac Low and A. P. Ingersoll, *Icarus* **65**, 353 (1986).
38. J. Sommeria *et al.*, *Nature* **331**, 689 (1988).
39. S. V. Antipov *et al.*, *ibid.* **323**, 238 (1986).
40. A. Hatzes *et al.*, *J. Geophys. Res.* **86**, 8745 (1981).
41. S. L. Hess and H. A. Panofsky, in *Compendium of Meteorology*, T. F. Malone, Ed. (American Meteorological Society, Boston, 1951), pp. 391–398.
42. A. P. Ingersoll and J. N. Cuzzi, *J. Atmos. Sci.* **26**, 981 (1969).
43. R. J. Terrile and J. A. Westphal, *Icarus* **30**, 247 (1977); R. J. Terrile and R. F. Beebe, *Science* **204**, 948 (1979).
44. G. P. Williams, *Nature* **257**, 778 (1975); *J. Atmos. Sci.* **35**, 1399 (1978).
45. L. A. Sromovsky *et al.*, *J. Atmos. Sci.* **39**, 1433 (1982).
46. K. G. Libbrecht, *Astrophys. J.* **336**, 1092 (1989).
47. C. Avis and S. A. Collins, *Voyager Time Lapse Cylindrical Projection Mosaics, JPL D-541* (Jet Propulsion Laboratory, Pasadena, CA, 1983), on 16-mm film.

48. This work was supported by the NASA Planetary Atmospheres Program and by Voyager Project funds. Contribution number 4824 from the Division of Geological and Planetary Sciences, California Institute of Technology.